IEEE Access
Multidisciplinary | Rapid Review | Open Access Journal

Received 17 August 2023, accepted 30 August 2023, date of publication 4 September 2023, date of current version 11 October 2023.

Digital Object Identifier 10.1109/ACCESS.2023.3311520

RESEARCH ARTICLE

Sequential Distributed Model Predictive Control for Automated Mining Fleet

ZHICHAO WANG AND JUE YANG
School of Mechanical Engineering, University of Science and Technology Beijing, Beijing 100083, China
Corresponding author: Jue Yang (yangjue@ustb.edu.cn)

This work was supported by the Ministry of Science and Technology of the People's Republic of China under Grant 2018YFC0604402.

ABSTRACT This work mainly focuses on fleet collaborative control for autonomous mining fleets. In this paper, we first developed a double-layer coupling model including the intersection platoon (IP) in the upper layer and the following platoon (FP) in the lower layer and unified the headway calculation and the structure of the control problem of the two types of platoons. Then, the constant time headway (CTH) spacing policy is implemented to ensure safety during fleet operation. Next, a controller based on the sequential distributed model predictive control (SEQ_DMPC) algorithm is proposed to solve the platoon control problem. To verify the proposed controller, we built a second-order electric truck longitudinal dynamics model as the actuators and verified the accuracy of the model. Next, we assume that all trucks are permitted to implement optimization simultaneously at each time step in the simulation and verify the platoon following stability based on the electric truck dynamic model. Finally, we simulated the fleet production process, and the results show that the proposed controller performs well in all aspects.

INDEX TERMS Autonomous vehicles, distributed control, intelligent transportation systems, predictive models, traffic control.

I. INTRODUCTION

In large open-pit mines, transportation costs account for more than 60% of the overall mine costs [1], and energy consumption accounts for more than half of the transportation costs [2]. Therefore, reducing energy consumption plays a vital role in reducing mine production costs and improving the revenue of open pit mines. During the operation of mining trucks, energy waste occurs in two main ways: 1. The truck's actual trajectory deviates significantly from the desired speed trajectory due to the weather, road condition, truck condition, or other influences, thus causing more energy consumption during the operation process. 2. Additional braking and acceleration maneuvers are taken by trucks to avoid traffic conflicts at intersections, which contribute more energy consumption. Therefore, solving the problems mentioned above is important to reduce fleet energy consumption as well as mining production costs.

The associate editor coordinating the review of this manuscript and approving it for publication was Qiang Li.

In open-pit mining production, the transportation tasks for each truck are assigned in advance by the dispatch system. When the transportation fleet consists of automated trucks, the optimal speed trajectory of the trucks can also be predefined in the dispatch system and combined with the fleet transportation tasks to generate the operating schedule with optimal efficiency and fuel consumption. Therefore, in the actual production process, fleet productivity and energy consumption can be optimized if the mine fleet can strictly follow the operating schedule.

At present, the studies for eliminating traffic conflicts in closed areas are mainly focused on the AGV fleet in container terminals [3], [4] or logistics parks [5], [6], [7], [8] and train formation in railway networks [9], [10], [11]. The main solutions for AGV fleets are mainly predicting potential traffic conflicts and thus changing the trajectory of the involved vehicles. For the management of train formations, the main solutions consist of the following steps: First, the transportation paths are divided into multiple sections according to a fixed length. Meanwhile, the intersection area and its adjacent paths are also treated as sections. Next, the priority of train

© 2023 The Authors. This work is licensed under a Creative Commons Attribution-NonCommercial-NoDerivatives 4.0 License.
For more information, see https://creativecommons.org/licenses/by-nc-nd/4.0/

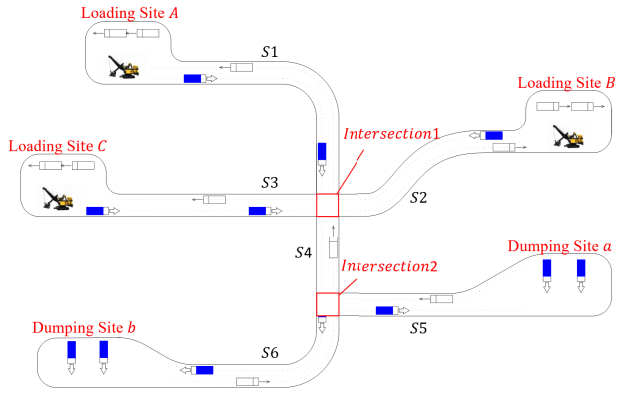

FIGURE 1. Schematic of the open-pit mine transportation path network.

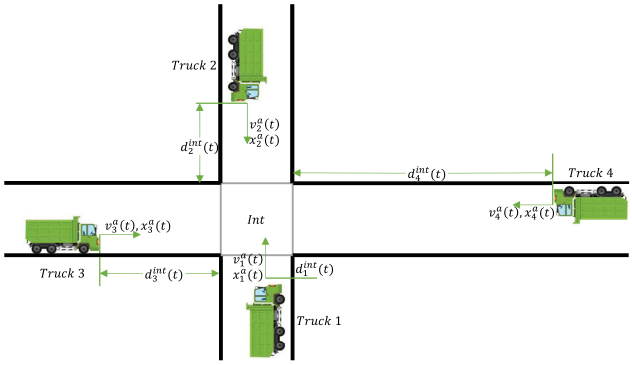

FIGURE 2. Example of IP.

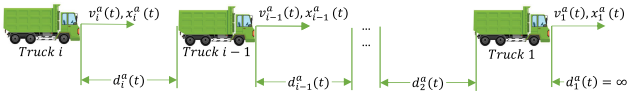

FIGURE 3. Example of FP.

formation is determined through certain rules. After that, the relevant railway section is locked to prevent other trains from entering, thus avoiding traffic conflicts. However, there are some shortcomings of current studies: the objective of the existing algorithms is to avoid traffic conflicts between vehicles or trains without considering saving energy consumption. This solution for AGVs tends to make the vehicle take on more braking and restarting processes, resulting in more energy consumption. At the same time, the solutions for train formation are unable to maximize railway utilization, and reduce transportation efficiency. For mining trucks, the curb mass and load capacity are extremely large, and the change in speed trajectory has a huge impact on energy consumption. Hence, the analysis of truck energy consumption mechanisms cannot be ignored when designing the mining transportation fleet control algorithm.

Fig. 1 shows a schematic diagram of the production and transportation path network of an open-pit mine. In the network, all platoons can be classified into two categories according to the path section on which the trucks are located, namely intersection platoon (IP) and following platoon (FP). IP refers to the queue of all trucks that are about to cross the same intersection, as shown in Fig. 2. Such platoon control issues are the focus of attention for the abovementioned AGV fleet control issues and train formation issues. FP refers to the queue formed by all vehicles sequentially arranged within the same path section, as shown in Fig. 3, and typical scenarios follow queues on highways [12], [13]. The objective of the problems is to reduce the overall fleet energy consumption while maintaining the desired spacing and speeds within the fleet. However, in the open pit mining fleet operation process, the relative spacing, speed, and energy consumption of the fleet need to be considered at the same time. Therefore, in this paper, we unified the IP control problem into the FP control problem, which not only ensures the safety of the IP through the intersection but also enables the platoon to maintain the established speed trajectory and achieve optimal energy consumption.

Research on the FP operation process can be traced back as far as the PATH project in the 1980s [14]. The program proposed an integrated longitudinal and lateral control algorithm for the operation of automated trucks in platoons, with an experiment using eight trucks on a two-lane freeway. The research content includes the control target of the platoon, sensing, and execution, and the solution framework of the fleet collaboration algorithm is also proposed. Since then, the problem of cooperative fleet control has received extensive attention and has yielded rich results in terms of air drag reduction [13], fleet stability [15], communication topology [16], and fleet operational safety [17].

The fleet collaborative controller is divided into a lower controller and an upper controller [18], where the lower controller is responsible for the truck dynamics control, aiming to make the trucks complete the path tracking according to the given trajectory, while the upper controller is the fleet controller, aiming to achieve the collaborative control of the fleet with the goal of optimal energy efficiency of the fleet under the premise of ensuring the safety of the fleet operation by giving the target position, target speed, and target acceleration information of all trucks. The upper controller is the core part of the whole fleet collaborative controller, which mainly contains three parts: fleet spacing policy, communication topology, and fleet operation controller.

The spacing policy is used to describe the relative positions of different trucks in a platoon. Each truck must follow its preceding truck and satisfy the relative spacing defined by the spacing policy. There are usually two types of spacing strategies: the constant spacing strategy (CSP) [19] and the variable spacing strategy (VSP) [20]. CSP is the simplest and most commonly used strategy. Compared to CSP, the desired distance in VSP varies with truck speed and can improve road transport efficiency [21]. To ensure fleet stability, VSP

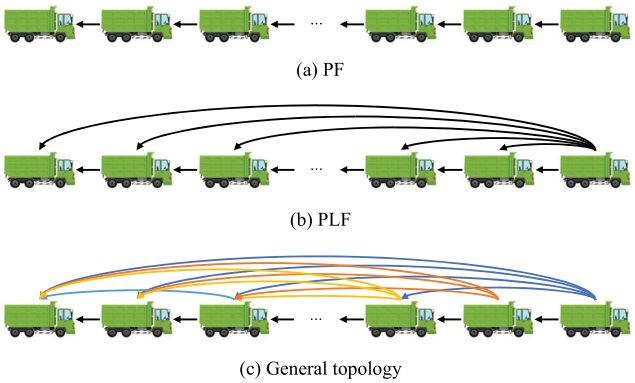

FIGURE 4. Communication topology type.

requires a minimum time spacing, called constant time headway (CTH) [22].

The communication topology ensures the integrity of the information flow and determines the design of the fleet controller. Lyapunov controller stability does not guarantee the stability of the platoon [23]. Errors and delays can be amplified as they travel with the platoon. This will lead to a worsening energy economy and even rear-end collisions. The most commonly used communication topologies are predecessor following (PF) [15], [18], predecessor-leader following (PLF) [24], general topologies [25], and other hybrid topologies [26], as shown in Fig. 4. Research shows that the PF communication topology does not guarantee the stability of the vehicle platoon [27], [28]. PLF can ensure platoon stability [29], as the information of the lead vehicle has a great impact on the stability of the fleet operation [30]. Furthermore, researchers have also given solutions for time delays [31] and dropout [26] to compensate for the drawbacks of communication characteristics.

Fleet operation controllers have matured over decades of development. The main control methods currently include PID control [31], robust control [32], sliding mode control [33], machine learning [34], and model predictive control [35]. Compared with other control methods, model predictive control (MPC) is not only effective in overcoming the uncertainty and nonlinearity of fleet systems but also more convenient in dealing with various constraints on the system state variables and control variables. Therefore, MPC has been widely used in various fields since it was proposed in the 1970s [36]. However, fleet cooperative control systems, as large systems with more complex coupling and numerous constraints, lead to too many decision variables for predictive control, which causes difficulties for the controller solution. At the same time, the geographical dispersion of the fleet also makes centralized control of the fleet difficult. These factors have promoted the development of distributed model predictive control [37]. Kianfar et al. [38] added the target of minimizing the controller output into the objective functions, as well as minimizing the status error and control error, to ensure the smoothness of the vehicle's operation. Thereafter, terminal constraints on status and control errors [29] and fluctuations of errors [39] are also added to the objective function to further improve the smoothness of the vehicle. Dai et al. [40] added the deviation of distance between the target vehicle and the preceding vehicle to the objective, which further improved the fleet operation efficiency by maintaining fleet spacing while ensuring smooth vehicle operation. However, with the continuous complexity of the objective function, especially when the objective function has multiple dimensional objectives, it is necessary to set weights for different objectives and find the optimal solution. Therefore, a large number of computational resources are needed, which leads to the degradation of the real-time performance of the algorithm. To solve this problem, Kianfar et al. [39] designed the multiobjective MPC (MOMPC) algorithm with the objectives of vehicle economy, safety, and stability by using Pontryagin's maximum principle (PMP). Zavala and Flores-Tlacuahuac [41] designed the utopia point based on the Pareto optimality, solved the multiobjective problem, and selected the Pareto optimal objective.

However, the current research mainly focuses on road freight truck queues, while there is a paucity of truck fleets for open pit mines. The main differences between the two are as follows: 1. Road freight trucks operate in an open road network, where there are a large number of other vehicles and random factors, and it is impossible to grasp real-time information of all vehicles in the network, so it is also impossible to completely avoid possible traffic conflicts during operation and to make a complete prediction of the fleet operation process. In open pit mines, the transportation path network is a closed area, and the information of all trucks is known or predictable, so it is feasible to completely eliminate traffic conflicts. 2. As mentioned above, the information of all vehicles on the network is not available. The control objective of road freight truck queues is to reduce fleet energy consumption by minimizing vehicle spacing to reduce air resistance while ensuring platoon safety. Otherwise, in open-pit mines, all conflicts can be eliminated in advance, and an operational schedule can be obtained. Therefore, the control problem is focused on making all the trucks in the transportation path network operate according to the schedule, and the objective function is to minimize the deviation between the actual trajectory and command trajectory in the schedule.

In summary, existing research has the following shortcomings: 1. The objective functions of existing collaborative controllers for vehicle platoons are mainly to eliminate traffic conflicts without considering the energy consumption, which is crucial for reducing the production costs of open-pit mines. 2. The existing research on collaborative control is limited to local areas, and there is no relevant research on the real-time control of vehicle platoons on a large scale in open road networks or on a global scale in closed road networks. 3. There are major differences between open-pit mining trucks and road freight vehicles. Therefore, the existing control methods cannot be directly used for mining trucks. To the best of our

knowledge, research on real-time control of transportation fleets in open-pit mines has not yet been conducted.

In this paper, we design a fleet collaborative controller for real-time control of an autonomous open pit mine production fleet real-time control based on a mining dispatching system and fleet operation schedule. First, we design a two-layer fleet coupling model based on the characteristics of the path network, in which the upper model couples all trucks that will pass through the intersection (IP) and the lower model couples all trucks that are arranged backward and forward on the same path section (FP). Next, we determine the constant time headway (CTH) spacing policy according to the actual requirements of the mine production protocol to enable the fleet to have different minimum following distances at different speeds, which not only ensures the safety of the fleet but also improves transportation efficiency as much as possible. After that, we introduced the proposed fleet controller. To ensure the stability of the fleet operation, we use the general topology in Fig. 4(c). The input of the controller is the desired status and speed obtained from the schedule, and the objective is to minimize the status and control error. Finally, it gives the command speed of the truck. The algorithm is based on the sequential distributed model predictive control algorithm (SEQ_DMPC) [42].

The main contributions of this paper are as follows:

1) A double-layer couple model is proposed. This model can connect all trucks in the path network and thus control the whole fleet.

2) A novel fleet controller is designed, and the SEQ_DMPC algorithm is proposed. By implementing the proposed DMPC algorithm, both the recursive feasibility of the optimization problem and the platoon stability of the whole system are guaranteed.

This paper follows the following structure: In the second section, the truck dynamic model is first proposed. Then, we introduce the methods which are made up of three parts: the fleet coupling model, spacing policy, and the fleet controller. After that, we explain the parameters of the experiment, operational scenarios, and key performance indicators (KPIs) in the third section. Finally, the results using the proposed model are analyzed in the fourth section, and we derive conclusions and further work in the fifth section.

II. APPROACHING

A complete mining intelligent transportation system (ITS) framework is shown in Fig. 5. It includes a fleet dispatching system and a fleet real-time control system. The dispatching system is responsible for planning and assigning the operation tasks of the mining fleet and giving the fleet operation schedule. The schedule includes the transport paths and sequences of all trucks, as well as the desired trajectory and input control at each moment within the transport shift. The real-time control system determines the optimal input control of the trucks at the next moment based on the current real-time status. Afterwards, optimal input control is used as an input to the truck dynamic control, and the latest state is updated after the simulation of the dynamics model. In this paper, we mainly focus on the fleet collaborative controller (upper controller) in the fleet real-time control system. We introduce the architecture of the controller in this section. At the same time, to verify the performance of the controller, we also established a truck dynamics controller (lower controller). In this chapter, we first introduce the electric truck dynamic model as the basis of the lower controller. Then in the second part, we present the framework of the fleet collaborative controller, which includes the fleet coupling model, spacing policy and proposed SEQ_DMPC controller algorithm.

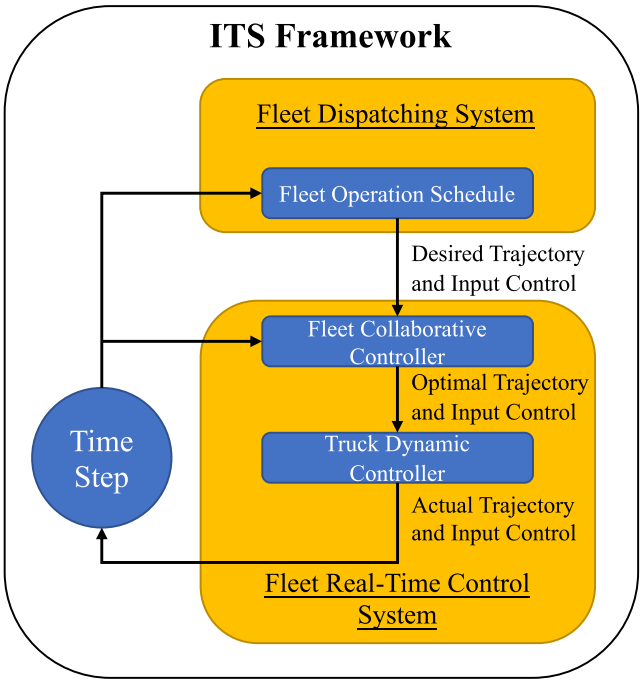

FIGURE 5. Framework of ITS.

A. MODEL OF ELECTRIC TRUCK DYNAMIC

In this paper, a second-order longitudinal truck dynamics model for electric trucks is used for the optimal control algorithm and simulation. To strike a balance between accuracy and simplicity, we make the following assumptions:

1) The body is rigid and symmetric from left to right;

2) The truck is on a flat and dry road surface, and the longitudinal tire slip is neglected;

3) Drive and brake torques are integrated into one single control input.

4) Only longitudinal dynamics are considered and not lateral dynamics.

Let $x(t)$, $v(t)$, $\mathrm{acc}(t)$ denote the position, longitudinal speed and acceleration of the truck, respectively. Then, the truck dynamics are represented by:

$$\dot{x}(t) = v(t) \tag{1}$$

$$\dot{v}(t) = \mathrm{acc}(t) \tag{2}$$

To use this dynamic model within our optimization, the dynamics are discretized in time, using a forward Euler approximation for v and x in (3) and (4).

$$v(k+1) = v(k) + \text{acc}(k)\,\Delta t \tag{3}$$

$$x(k+1) = x(k) + v(k)\,\Delta t + \text{acc}(k)\,\Delta t^2/2 \tag{4}$$

where Δt is the time step.

When the speed and acceleration of the truck are determined, the longitudinal force required for the truck is given in (5):

$$F_{long} = M\text{acc} + F^{roll} + F^{wind} + F^{grd} \tag{5}$$

where M is the mass of the truck and F^{roll}, F^{wind} and F^{grd} are the rolling resistance, wind resistance, and slope resistance, respectively, and are presented in (6) to (8).

$$F^{roll}(t) = MgC_{roll}\cos\alpha(t) \tag{6}$$

$$F^{wind} = \rho A_w C_w v^2(t)/2 \tag{7}$$

$$F^{grd} = Mg\alpha(t) \tag{8}$$

where g is the gravity acceleration, C_{roll} is the rolling resistance coefficient, $\alpha(t)$ is the slope of the position in the transportation path where the truck is located at time t, ρ is the air density, A_w is the windward area of the truck, and C_w is the wind resistance coefficient.

For both the optimizations and simulations, we assume that the output power of the motor is known based on the motor torque and motor speed. Thus, propulsive force and speed need to be converted to motor torque and speed in (9) and (10).

$$T^{mot} = F_{long} r_{wh}/i_g i_a \tag{9}$$

$$\omega^{mot} = v i_g i_a / r_{wh} \tag{10}$$

where r_{wh} is the rolling radius of the truck's tires, i_g is the gear ratio, and i_a is the final drive ratio.

Finally, the output power of the motor is calculated in (11).

$$P^{mot} = F_{long} v \tag{11}$$

Moreover, when the units of P^{mot}, T^{mot} and ω^{mot} are kW, Nm and rpm respectively, the calculation of P^{mot} can be given as follows:

$$\begin{aligned} P^{mot} &= F_{long} 2\pi r_{wh} \omega^{mot} i_g i_a / 60 / 1000 \\ &= 2\pi / 60000 F_{long} r_{wh} i_g i_a \omega^{mot} \\ &\approx 9549 T^{mot} \omega^{mot} \end{aligned} \tag{12}$$

B. FRAMEWORK OF FLEET COLLABORATIVE CONTROLLER

In this section, we present our proposed real-time fleet control algorithm. First, to include all trucks in the controller, we first design a two-layer fleet coupling model, which treats all IPs in the transportation path network as the so-called upper platoon and all FPs as the lower platoon. Then, we transform the IP control problem into an FP control problem, so that a unified computational framework can be used to solve the control of both platoons. Next, we introduce the spacing policy. According to the requirements of the actual production regulations of the open pit mine, we adopt the CTH spacing policy, which makes the fleet have different spacing requirements at different speeds, ensuring the safety of the fleet operation and improving the efficiency of the fleet at the same time. Finally, we present our proposed sequential model predictive control algorithm, including the problem construction, objective function and related constraints.

First, we introduce the definitions of some terms in this chapter.

Loading site: Place where a truck loads materials to be transported.

Dumping site: Place where the materials are dumped.

Path: Trucks traveled between loading sites and dumping sites.

Intersection: Place where two paths cross each other.

Section: Path between an intersection and a loading site, a dumping site or another intersection.

Direction: Truck running direction: 1 is from the loading site to the dumping site and 2 is from the dumping site to the loading site.

1) FLEET COUPLING MODEL

We classify the fleet in the path network into two categories: intersection platoon (IP) and following platoon (FP). We define the two types of platoons in *Definition 1* and *Definition 2* and define truck priority in *Definition 3*.

Definition 1: An intersection platoon (IP) refers to all trucks with a destination at the same intersection, denoted as IP_{int}, which means that the target intersection of the platoon is int. The number of IPs is equal to the number of intersections in the path network, with a maximum of four trucks for each IP.

In IP, as shown in Fig. 2, we denote $d_i^a(t)$ as the actual distance to the entrance of the intersection, and $v_i^a(t)$ as the actual speed of truck i at moment t.

Definition 2: Following platoon (FP) refers to all trucks travelling in one section in the same direction, denoted as FP_{sec}^{dir}, which means that the platoon drives on section sec, and the direction is dir. There are two FPs in each section.

In FP, as shown in Fig. 3, we denote $x_i^a(t)$ as the actual distance to the preceding truck, and $v_i^a(t)$ as the actual speed of truck i at moment t. When truck i is the leading truck in the platoon, we define $d_i^a(t) = \infty$.

Definition 3: In each platoon, there is a high or low priority of trucks, and we define that truck with high priority will not be affected by trucks with low priority.

In a platoon, we number the trucks according to their priority, specifying that the truck with the highest priority is numbered 1, and the larger the number is, the lower the priority of the truck in the platoon. In FP_{sec}^{dir}, the leading truck has the highest priority, as $Truck1$ in Fig. 3, and the truck immediately following the lead truck has the next highest priority, as $Truck2$ in Fig. 3 and so on. In IP_{int}, the truck priority is related to the distance of the truck from the intersection area. The truck closest to the intersection has the highest

priority, and vice versa. For example, in Fig. 2, if $d_1^{int}(t) < d_2^{int}(t) < d_3^{int}(t) < d_4^{int}(t)$, we number *Truck*1 as IP_{int} [1] and number *Truck*4 as IP_{int} [1].

2) SPACING POLICY

We set a minimum time headway t_{cth} as the time-headway spacing policy, which also belongs to a VSP, to follow the preceding truck with a desired minimum relative distance $d_i^d(t)$ between truck i and the preceding truck $i-1$ is defined as:

$$d_i^d(t) = t_{cth} v_i^a(t) \tag{13}$$

When the length of the truck is L, the actual distance $d_i^a(t)$ between truck i and the preceding truck $i-1$ in FP, as shown in fig.3, is calculated by (14):

$$d_i^a(t) = \begin{cases} x_i^a(t) - x_{i-1}^a, & i \in \{2, 3, 4, \ldots\} \\ \infty, & i = 1 \end{cases} \tag{14}$$

We assume that $d_1^{int}(t) < d_2^{int}(t) < d_3^{int}(t) < d_4^{int}(t)$ in IP; then, $d_i^a(t)$ is given by (15):

$$d_i^a(t) = \begin{cases} d_a^{int}(t) - d_{i-1}^{int}(t), & i \in \{2, 3, 4, \ldots\} \\ d_1^{int}(t), & i = 1 \end{cases} \tag{15}$$

During the fleet operation process, the actual spacing between trucks should not be less than the desired minimum relative distance in (16).

$$d_i^a(t) \geq d_i^d(t) \tag{16}$$

3) FLEET CONTROLLER BASED ON SEQUENTIAL DISTRIBUTED MODEL PREDICTIVE CONTROL (SEQ_DMPC) ALGORITHM

In our proposed SEQ_DMPC algorithm, at moment, for each truck, we denote:

1) N_p and N_c are the prediction horizon and control horizon, respectively.

2) $s_i(t)$ and $c_i(t)$ are the actual output trajectory and input control of truck i at moment t, respectively. They are obtained from the electric truck dynamic model and are known as quantities at moment t.

3) $s_{i,ref}(t)$ and $c_{i,ref}(t)$ are the reference trajectory and input control of truck i at moment t, respectively. They are obtained from the fleet operation schedule and are known as quantities at moment t.

4) $s_i\left(t' \mid t\right)$ and $c_i\left(t' \mid t\right)$ are the predictive output trajectory and input control of truck i at moment t' by the electric truck dynamic model when the current trajectory and input control are $s_i(t)$ and $c_i(t)$, respectively.

5) $c_i^*(t)$ is the optimal input control of truck i at moment t, which is obtained by SEQ_DMPC at moment $t - t_s$.

The system dynamics are discretized using the Euler method with sampling time t_s to obtain:

$$s_i(t + t_s) = A(t)\, s_i(t) + B(t)\, c_i(t) \tag{17}$$

We define the output trajectory deviation $S_i(t)$ and the input control deviation $U_i(t)$ as:

$$S_i(t) = s_i(t) - s_{i,ref}(t) \tag{18}$$

$$U_i(t) = c_i(t) - c_{i,ref}(t) \tag{19}$$

The deviation of the output trajectory can be rewritten as:

$$S_i(t + t_s) = A(t)\, S_i(t) + B(t)\, U_i(t) \tag{20}$$

Expanding the above equation according to the model prediction control sequence:

$$S_i\left(t' + t_s \mid t\right) = A(t)\, S_i\left(t' \mid t\right) + B(t)\, U_i\left(t' \mid t\right) \tag{21}$$

In addition, the reference trajectory $s_{i,ref}(t)$ and input control $c_{i,ref}(t)$ are obtained by the dispatching system, they also meet the system dynamics in (17), which is:

$$s_{i,ref}(t + t_s) = A(t)\, s_{i,ref}(t) + B(t)\, c_{i,ref}(t) \tag{22}$$

For truck i, the objective of the single truck control problem is to minimize the deviation of the output trajectory and input control within all prediction sequences while satisfying the constraints of status and control. The objective function of the control problem of truck i is defined in (23):

$$\begin{aligned} \min_{\{U_i(t)\},\in} J_i(t) = & \sum_{k=0}^{N_c} \left\| U_i(t + kt_s \mid t) \right\|_Q^2 + \rho\epsilon^2 \\ & + \sum_{k=1}^{N_p - 1} \left\| S_i(t + kt_s \mid t) \right\|_P^2 \\ & + \left\| S_i(t + kt_s \mid t) \right\|_F^2 \end{aligned} \tag{23}$$

$$\text{Subject to: } c_i(t \mid t) = c_i(t) \tag{24}$$

$$\begin{aligned} & c_i(t + kt_s \mid t) = c_{i,ref}(t + kt_s) \\ & + U_i(t + kt_s \mid t) \end{aligned} \tag{25}$$

$$\begin{aligned} & s_i(t + (k+1)\, t_s \mid t) \\ & = A(t + kt_s \mid t)\, s_i(t + kt_s \mid t) \\ & + B(t + kt_s \mid t)\, c_i(t + kt_s \mid t) \end{aligned} \tag{26}$$

$$c_{min} \leq c_i(t + nt_s \mid t) \leq c_{max} \tag{27}$$

$$\begin{aligned} & \Delta c_{min} \leq c_i(t + (n+1)\, t_s \mid t) \\ & - c_i(t + nt_s \mid t) \leq \Delta c_{max} \end{aligned} \tag{28}$$

$$S_i\left(t + N_p t_s \mid t\right) = 0 \tag{29}$$

$$\begin{aligned} & U_i(t) = [U_i(t \mid t), U_i(t + t_s \mid t), \\ & \ldots, U_i(t + N_c t_s \mid t)] \end{aligned} \tag{30}$$

$$N_p = N_c + 1 \tag{31}$$

$$\epsilon > 0 \tag{32}$$

where matrices Q, P and F are the weight matrices of input control error, output trajectory error and terminal output trajectory error, respectively.

After solving the above problem to obtain the sequence $U_i(t)$, the optimal input control of truck i at moment t is:

$$c_i^*(t) = c_{i,ref}(t) + U_i(t \mid t) \tag{33}$$

Next, we describe the method for constructing each problem. In this paper, we use SEQ_DMPC to solve the problem, and this type of solution method belongs to a class of collaborative DMPC [42].

For any platoon, we assume that there are n trucks at moment t in it and that all trucks have been numbered from 1 to n according to their priority. We denote the objective function of truck m as $J_m(t)$ in (23) and the optimal control problem of truck m as $DMPC_m$. Then, the solving strategy of each platoon is shown as follows:

1) At moment t, the current output trajectory $s_i(t)$, desired output trajectory $s_{i,ref}(t)$ and actual input control $c_i(t)$ of all trucks are known.

2) Make $m = n$:

a) Solve the problem $DMPC_m$, and the objective function of the problem is given by:

$$\min_{\{U_1(t)\},\{U_2(t)\},\ldots,\{U_m(t)\}} J_{DMPC_m}(t) = \sum_{i=m}^{1} J_i(t) \tag{34}$$

b) Obtain the solution $\{U_1(t)\}, \{U_2(t)\}, \ldots, \{U_m(t)\}$.

c) Obtain the optimal input control of truck m:

$$c_m^*(t) = c_{m,ref}(t) + U_m(t \mid t) \tag{35}$$

d) If $m = 1$, stop the algorithm. Otherwise, make $m = m - 1$, and return to step a).

When solving the problem, not only should the constraints (24) to (32) be satisfied but it is also necessary to satisfy the spacing policy in (16) between different trucks in the platoon.

Fig.6 shows the solution framework of the fleet controller. In the part of the fleet coupling model, all trucks in the IP are the leading trucks in the corresponding FP. The priority of trucks in all IPs is higher than that of trucks in FP. Therefore, we first solve the control problems for all IPs using the strategy above. After that, the optimal input control of all the leading trucks in FPs are known, and the control problems $DMPC_1$ in all FPs are ignored. Only the control problems of other trucks need to be solved by using the same strategy we proposed.

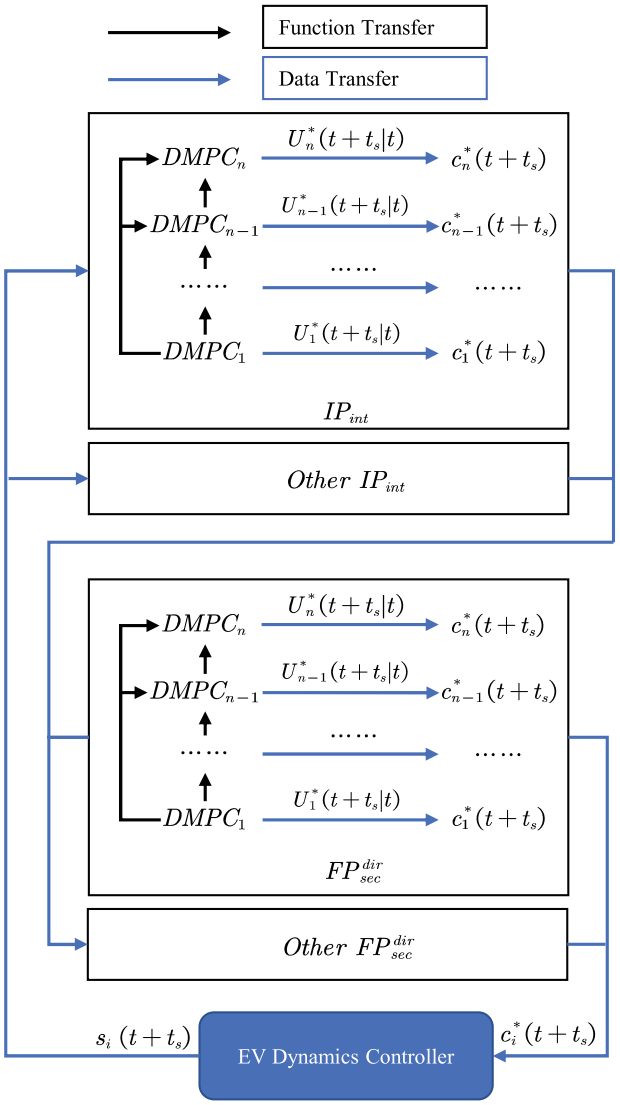

FIGURE 6. Fleet controller framework.

4) STABILITY AND FEASIBILITY ANALYSIS

At moment t, the optimal solution sequence $\{U_i^*(t)\}$, optimal input control sequence $\{c_i^*(t)\}$, and optimal predicted trajectory sequence $\{s_i^*(t)\}$ of the control problem are as follows:

$$\begin{aligned}
\{U_i^*(t)\} &= \left[U_i^*(t \mid t), U_i^*(t+t_s \mid t), \ldots, U_i^*(t+N_c t_s \mid t)\right] \\
\{c_i^*(t)\} &= \left[c_i^*(t \mid t), c_i^*(t+t_s \mid t), \ldots, c_i^*(t+N_c t_s \mid t)\right] \\
\{s_i^*(t)\} &= \left[s_i^*(t+t_s \mid t), \ldots, s_i^*(t+N_c t_s \mid t), \right. \\
&\qquad \left. s_i^*\left(t+N_p t_s \mid t\right)\right]
\end{aligned} \tag{36}$$

All components of the sequences above satisfy the constraints from (24) to (32).

Without considering noise, the actual trajectory $s_i(t+t_s)$ and actual input control $c_i(t+t_s)$ of the system are as follows:

$$s_i(t+t_s) = s_i^*(t+t_s \mid t) \tag{37}$$

According to (29), the predicted terminal trajectory and the optimal terminal trajectory are the same as the reference trajectory.

$$s_i\left(t+N_p t_s \mid t\right) = s_i^*\left(t+N_p t_s \mid t\right) = s_{i,ref}\left(t+N_p t_s\right) \tag{38}$$

At moment t, we assume that the objective function corresponding to the optimal solution of control problem (23) for truck i is $J_i^*(t)$, the objective function corresponding to the feasible solution is $J_i(t)$, and the relation of $J_i^*(t)$ and $J_i(t)$ is expressed by (39).

$$J_i^*(t) \le J_i(t) \tag{39}$$

Similarly:

$$J_i^*(t+t_s) \le J_i(t+t_s) \tag{40}$$

Subtract $J_i^*(t)$ on both sides of (40) simultaneously, and we donate:

$$J_i^*(t+t_s) - J_i^*(t) \le J_i(t+t_s) - J_i^*(t) = l_P + l_F + l_Q \tag{41}$$

where:

$$\begin{aligned} l_P &= \sum_{k=1}^{N_p-1} \left\| s_i(t+t_s+kt_s \mid t+t_s) - s_{i,ref}(t+t_s+kt_s) \right\|_P^2 \\ &\quad - \sum_{k=1}^{N_p-1} \left\| s_i^*(t+kt_s \mid t) - s_{i,ref}(t+kt_s) \right\|_P^2 \end{aligned} \tag{42}$$

$$\begin{aligned} l_F &= \left\| s_i\left(t+t_s+N_pt_s \mid t+t_s\right) - s_{i,ref}\left(t+t_s+N_pt_s\right) \right\|_F^2 \\ &\quad - \left\| s_i^*\left(t+N_pt_s \mid t\right) - s_{i,ref}\left(t+N_pt_s\right) \right\|_F^2 \end{aligned} \tag{43}$$

$$\begin{aligned} l_Q &= \sum_{k=0}^{N_c} \left\| c_i^*(t+kt_s \mid t) - c_{i,ref}(t+kt_s) \right\|_Q^2 \\ &\quad - \sum_{k=0}^{N_c} \left\| c_i^*(t+kt_s \mid t) - c_{i,ref}(t+kt_s) \right\|_Q^2 \end{aligned} \tag{44}$$

Further derivation of equations (42) to (44) yields:

$$\begin{aligned} l_P &= \sum_{k=1}^{N_p-1} \left\| s_i(t+t_s+kt_s \mid t+t_s) - s_{i,ref}(t+t_s+kt_s) \right\|_P^2 \\ &\quad - \sum_{k=1}^{N_p-1} \left\| s_i^*(t+kt_s \mid t) - s_{i,ref}(t+kt_s) \right\|_P^2 \\ &= \sum_{k=1}^{N_p-2} \left\| s_i(t+t_s+kt_s \mid t+t_s) - s_{i,ref}(t+t_s+kt_s) \right\|_P^2 \\ &\quad + \left\| s_i\left(t+t_s+\left(N_p-1\right)t_s \mid t+t_s\right) \right. \\ &\quad \left. - s_{i,ref}\left(t+t_s+\left(N_p-1\right)t_s\right) \right\|_P^2 \\ &\quad - \sum_{k=1}^{N_p-1} \left\| s_i^*(t+kt_s \mid t) - s_{i,ref}(t+kt_s) \right\|_P^2 \\ &= \sum_{k=1}^{N_p-1} \left\| s_i^*(t+kt_s \mid t) - s_{i,ref}(t+kt_s) \right\|_P^2 \\ &\quad - \sum_{k=1}^{N_p-1} \left\| s_i^*(t+kt_s \mid t) - s_{i,ref}(t+kt_s) \right\|_P^2 \\ &\quad + \left\| s_i\left(t+t_s+\left(N_p-1\right)t_s \mid t+t_s\right) \right. \\ &\quad \left. - s_{i,ref}\left(t+t_s+\left(N_p-1\right)t_s\right) \right\|_P^2 \\ &= \left\| s_i\left(t+t_s+\left(N_p-1\right)t_s \mid t+t_s\right) \right. \\ &\quad \left. - s_{i,ref}\left(t+t_s+\left(N_p-1\right)t_s\right) \right\|_P^2 \\ &\quad - \left\| s_i^*(t+t_s \mid t) - s_{i,ref}(t+t_s) \right\|_P^2 \\ &= \left\| s_i^*\left(t+N_pt_s \mid t\right) - s_{i,ref}\left(t+N_pt_s\right) \right\|_P^2 \\ &\quad - \left\| s_i^*(t+t_s \mid t) - s_{i,ref}(t+t_s) \right\|_P^2 \le 0 \end{aligned} \tag{45}$$

$$\begin{aligned} l_F &= \left\| s_i\left(t+t_s+N_pt_s \mid t+t_s\right) - s_{i,ref}\left(t+t_s+N_pt_s\right) \right\|_F^2 \\ &\quad - \left\| s_i^*\left(t+N_pt_s \mid t\right) - s_{i,ref}\left(t+N_pt_s\right) \right\|_F^2 = 0 \end{aligned} \tag{46}$$

$$\begin{aligned} l_Q &= \sum_{k=0}^{N_c} \left\| c_i(t+t_s+kt_s \mid t+t_s) - c_{i,ref}(t+t_s+kt_s) \right\|_Q^2 \\ &\quad - \sum_{k=0}^{N_c} \left\| c_i^*(t+kt_s \mid t) - c_{i,ref}(t+kt_s) \right\|_Q^2 \\ &= \sum_{k=0}^{N_c-1} \left\| c_i(t+t_s+kt_s \mid t) - c_{i,ref}(t+t_s+kt_s) \right\|_Q^2 \\ &\quad + \left\| c_i(t+(N_c+1)t_s \mid t+t_s) - c_{i,ref}(t+(N_c+1)t_s) \right\|_Q^2 \\ &\quad - \sum_{k=0}^{N_c} \left\| c_i^*(t+kt_s \mid t) - c_{i,ref}(t+kt_s) \right\|_Q^2 \\ &= \sum_{k=1}^{N_c} \left\| c_i^*(t+kt_s \mid t) - c_{i,ref}(t+kt_s) \right\|_Q^2 \\ &\quad - \sum_{k=0}^{N_c} \left\| c_i^*(t+kt_s \mid t) - c_{i,ref}(t+kt_s) \right\|_Q^2 \\ &\quad + \left\| c_i(t+(N_c+1)t_s \mid t+t_s) - c_{i,ref}(t+(N_c+1)t_s) \right\|_Q^2 \\ &= \left\| c_i(t+(N_c+1)t_s \mid t+t_s) - c_{i,ref}(t+(N_c+1)t_s) \right\|_Q^2 \\ &\quad - \left\| c_i^*(t \mid t) - c_{i,ref}(t) \right\|_Q^2 \end{aligned} \tag{47}$$

According to (37), we expand $s_i^*\left(t+t_s+N_pt_s \mid t+t_s\right)$ and $s_{i,ref}\left(t+t_s+N_pt_s\right)$ with the system dynamic in (17) as follows:

$$\begin{aligned} &s_i^*\left(t+t_s+N_pt_s \mid t+t_s\right) \\ &\quad = A(t+t_s+N_ct_s)\, s_i^*(t+t_s+N_ct_s \mid t) \\ &\qquad + B(t+t_s+N_ct_s)\, c_i^*(t+t_s+N_ct_s \mid t) \\ &\quad = s_{i,ref}\left(t+t_s+N_pt_s\right) \\ &\quad = A(t+t_s+N_ct_s)\, s_{i,ref}(t+t_s+N_ct_s) \\ &\qquad + B(t+t_ss+N_ct_s)\, c_{i,ref}(t+t_s+N_ct_s) \end{aligned} \tag{48}$$

Reorganizing the above formula yields:

$$\begin{aligned} &B(t+t_s+N_ct_s)\left(c_{i,ref}(t+t_s+N_ct_s)\right. \\ &\quad \left. - c_i^*(t+t_s+N_ct_s \mid t+t_s)\right) \\ &= A(t+t_s+N_ct_s) \\ &\quad \times \left(s_i^*(t+t_s+N_ct_s \mid t+t_s) - s_{i,ref}(t+t_s+N_ct_s)\right) \end{aligned} \tag{49}$$

Hence:

$$\begin{aligned} l_Q &= \left\| c_i(t+t_s+N_ct_s \mid t+t_s) - c_{i,ref}(t+t_s+N_ct_s) \right\|_Q^2 \\ &\quad - \left\| c_i^*(t \mid t) - c_{i,ref}(t) \right\|_Q^2 \\ &= - \left\| c_i^*(t \mid t) - c_{i,ref}(t) \right\|_Q^2 \le 0 \end{aligned} \tag{50}$$

Substituting (45), (46), and (50) into (41) yields:

$$J_i(t+t_s) - J_i^*(t) \le 0 \tag{51}$$

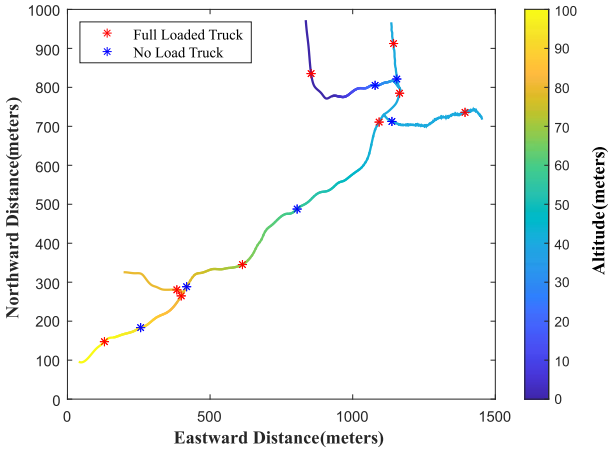

FIGURE 7. Transportation path network of the open pit coal mine.

TABLE 1. Parameters of the mining path network.

Path	Length(m)	Ramp length(m)	Maximum continuous ramp length(m)
A to a	2825.2	1256.2	905
A to b	2820.6	1507.5	905
B to a	2819.4	1005.0	905
B to b	2826.5	1256.2	905
C to a	2820.8	1507.5	905
C to b	2822.0	1758.7	905

For control problem $DMPC_1$, there is:

$$J_{DMPC_m}(t+t_s) = \sum_{i=m}^{1} J_i(t+t_s) \leq \sum_{i=m}^{1} J_i(t) = J_{DMPC_m}(t) \tag{52}$$

Therefore, the problem is asymptotically stable. At the same time, in order to ensure the asymptotic stability of the problem (34), it is necessary to add terminal constraints to the objective function in (29).

III. DESIGN OF EXPERIMENTS

A. PARAMETERS

1) PARAMETERS OF THE OPEN-PIT MINE TRANSPORTATION PATH NETWORK

We consider the transportation fleet in a transportation network of an open-pit coal mine in China. For confidentiality reasons, we only provided the relative position of the network without real location information, and the network is shown in Fig.7. There are three loading sites (A, B and C) and two dumping sites (a and b) as well as three intersections in the entire path network. In this network, there is only one connecting path between each loading site and each dumping site, which is the transportation path. Therefore, there are a total of six transportation paths in this network. The related information is shown in Table 1.

According to the mining operation regulations, the slope of the transportation path is not greater than 8%, and the actual slope measurement is between 7% and 8.5%. We set the slope of all transportation paths to 8%. At the same time, the operation regulations require that the minimum following distance on the transport path shall not be less than 100 m, the stopping minimum following distance shall not be less than 50 m, and the speed limit for trucks with no load is 50 km/h, and 35 km/h for full load. According to (13), the minimum time headway is 7.2 s. To ensure the safety and stability of fleet operation, in this paper, we set t_{cth} equals 5 s.

2) PARAMETERS OF THE ELECTRIC TRUCK

In this paper, we have established a dynamic model for the TR50E mining truck, and the parameters of the truck are listed in Table 2.

B. EXPERIMENTAL SCENARIOS

In this paper, we deploy an electric truck fleet in a mining transportation path network and use our designed SEQ_DMPC algorithm to dynamically control and simulate fleet operation. The quality of the truck dynamics model has a significant impact on the production indicators of fleet transportation, and it also affects the evaluation of the real-time control algorithm performance of the fleet. Therefore, to verify the performance of our fleet control algorithm, we first verify the accuracy of the electric truck model. Afterwards, we verified the operational stability of the platoons mentioned under the designed algorithm proposed in this paper. Finally, we conducted a complete simulation of the transportation process of one shift of the transportation fleet in the transportation path network to verify the algorithm for the fleet.

1) VERIFICATION OF THE ELECTRIC TRUCK DYNAMIC MODEL

The speed trajectory following verification of the dynamic model of electric trucks mainly includes speed following performance, acceleration and deceleration performance. The conditions for truck operation are divided into uphill, flat, and downhill conditions. At the same time, we believe that mining trucks do not actively accelerate or decelerate during uphill or downhill processes. For this purpose, we designed a custom expected speed trajectory to validate the dynamic model we established. This speed trajectory includes all possible operating conditions of mining trucks. The initial status of the truck is set to $x_i(0) = 0$; $v_i(0) = 0$, and the desired speed trajectory is given in Fig.8. Then, we verified the following performance of the dynamics model for the optimal speed trajectory in the mining transportation paths. The travel times of the optimal speed trajectories for trucks on different paths are shown in Table 3.

2) VERIFICATION OF PLATOON FOLLOWING CONTROLLER STABILITY

In this part, we verify the platoon following stability in which the following trucks can adjust their speed accordingly when

TABLE 2. Parameters of TR50E electric truck.

Parameters	Value	Unit
Body length	8.875	m
Body width	4.27	m
Body height	4.345	m
Spread of axles	3.96	m
Curb weight	37	t
Load capacity	45	t
Height of empty centroid	2.0	t
Height of full load centroid	2.55	m
Distribution of rear axle load with empty	52	%
Distribution of rear axle load with full load	66	%
Frontal area	2.2	m^2
Tire rolling radius	0.94	m
Adhesion coefficient	0.6	
Full load speed limit	35	km/h
No load speed limit	50	km/h
Full load acceleration limit	0.6	m/s^2
No load acceleration limit	1.0	m/s^2
Transmission reduction ratio	5.53/3.05/1.66/1.00	
Final drive reduction ratio	17.829	
Transmission maximum input torque	2400	Nm
Transmission maximum input speed	3000	rpm
Motor rated power	320	kW
Motor maximum output power	450	kW
Motor rated torque	1605	Nm
Motor maximum output torque	2300	Nm

the leading truck suddenly slows down and maintain a safe distance or time headway due to unexpected reasons during the operation process. We designed two scenarios for the verification as follows:

1) The leading truck slows down suddenly for a short time period and is restored to the original speed.

2) The leading truck slows down suddenly and is unable to restore the original speed.

For each scenario, we considered a FP consisting of four electric mining trucks. In a FP, all trucks have the same loading status, so we verified an empty platoon and a full platoon in each scenario for a total 4 experiments. We numbered the trucks as 1, 2, 3 and 4 based on the definition of truck priority as shown in Fig.3.

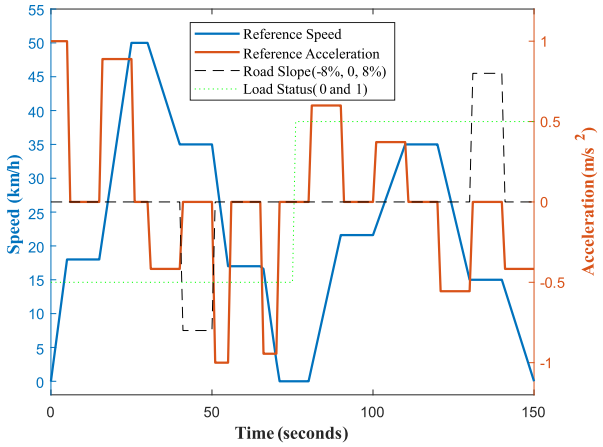

FIGURE 8. Custom desired speed trajectory of the electric truck dynamic model.

TABLE 3. Travel time of optimal speed trajectory in different paths.

Path	Travel time with full load(s)	Travel time with no load(s)
A to a	528.5	236
A to b	593	242
B to a	510	243
B to b	553	245
C to a	600	243
C to b	643	242

We denote v_i^{ref} as the desired speed trajectory of truck, and the desired speed trajectories for the full platoon and empty platoon in Scenario 1 are shown in (53) and (54), respectively.

$$v_0^{ref} = \begin{cases} 35 \text{ km/h} & t \le 10s \\ 20 \text{ km/h} & 10s < t \le 20s \\ 35 \text{ km/h} & t > 20s \end{cases}$$
$$v_i^{ref} = 35km/h \quad i = \{2, 3, 4\} \tag{53}$$

$$v_0^{ref} = \begin{cases} 50 \text{ km/h} & t \le 10s \\ 35 \text{ km/h} & 10s < t \le 20s \\ 50 \text{ km/h} & t > 20s \end{cases}$$
$$v_i^{ref} = 50 \text{ km/h} \quad i = \{2, 3, 4\} \tag{54}$$

The desired speed trajectories for the full platoon and empty platoon in Scenario 2 are shown in (55) and (56), respectively.

$$v_0^{ref} = \begin{cases} 35 \text{ km/h} & t \le 10s \\ 20 \text{ km/h} & t > 10s \end{cases}$$
$$v_i^{ref} = 35 \text{ km/h} \quad i = \{2, 3, 4\} \tag{55}$$

TABLE 4. Path index for electric mining truck fleet transportation task.

Transportation cycle	1		2		3	
Truck index	Full	Empty	Full	Empty	Full	Empty
1	6	4	3	3	3	5
2	5	3	3	1	1	5
3	5	3	3	3	3	5
4	5	3	3	3	3	5
5	5	3	3	3	3	5
6	2	4	3	1	2	2
7	4	2	1	5	5	3
8	4	2	1	5	5	3
9	1	1	2	4	3	1
10	1	3	4	6	5	1
11	1	1	1	5	6	2
12	1	1	1	5	5	1
13	1	1	1	5	5	1
14	3	5	6	4	3	3
15	3	5	5	1	1	3
16	3	5	5	1	1	3
17	3	5	5	1	1	3
18	3	5	5	1	1	3

Correspondence between path index and path in the table is shown below: 1: A to a; 2: A to b; 3: B to a; 4: B to b; 5: C to a; 6: C to b.

$$v_0^{ref} = \begin{cases} 50 \text{ km/h} & t \le 10s \\ 35 \text{ km/h} & t > 10s \end{cases}$$
$$v_i^{ref} = 50 \text{ km/h} \quad i = \{2, 3, 4\} \tag{56}$$

In the simulation, we set the minimum following time headway $t_{cth} = 5$s. At moment t, we denote the actual time headway and the actual distance between the following truck i and the preceding truck $i-1$ as $T_{i,i-1}(t)$ and $S_{i,i-1}(t)$. The calculation of $T_{i,i-1}(t)$ is given by:

$$T_{i-1,i}(t) = S_{i-1,i}(t) / v_i(t) \tag{57}$$

where $v_i(t)$ is the actual speed of truck i at moment t.

3) FLEET PRODUCTION SIMULATION

In the actual production process of open-pit mines, 18 electric mining trucks of the same model are involved in transportation operations. In this section, we simulate the transportation process of the fleet through three transportation cycles. All truck transportation task paths are shown in Table 4.

C. KEY PERFORMANCE INDICATORS (KPIs)

To evaluate the performance of our proposed SEQ_DMPC algorithm, we need to use some key performance indicators (KPIs). The important KPIs, based on which we evaluate the performance of our model in the next subsections, are listed in Table 5.

The explanations of the KPIs are as follows:

1) Speed error at time t: The difference between the actual truck speed and the desired speed at moment t.

TABLE 5. Key performance indicators.

KPI	Units
Speed error at moment t	m/s
Speed error at distance s	m
Time headway	s
Distance delay	m
Time delay	s

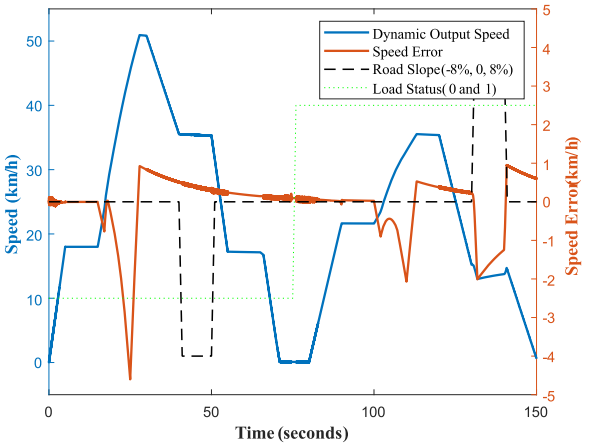

FIGURE 9. Actual speed and speed error of the EV dynamic model.

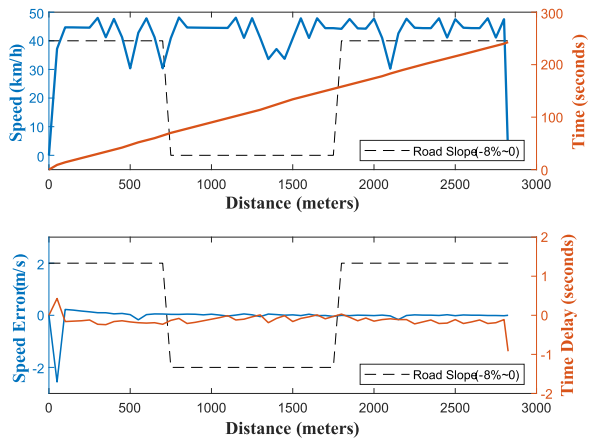

FIGURE 10. Optimal speed trajectory following performance with no load.

2) Speed error at distance s: The difference between the actual truck speed and the desired speed when the truck is located in position s.

3) Distance delay: The difference between the actual position of the truck and the desired position at moment t.

4) Time delay: The difference between the actual time of the truck and the desired time when the truck reaches position s.

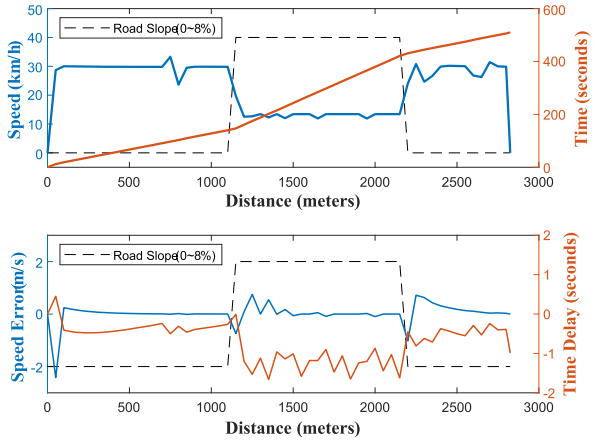

FIGURE 11. Optimal speed trajectory following performance with full load.

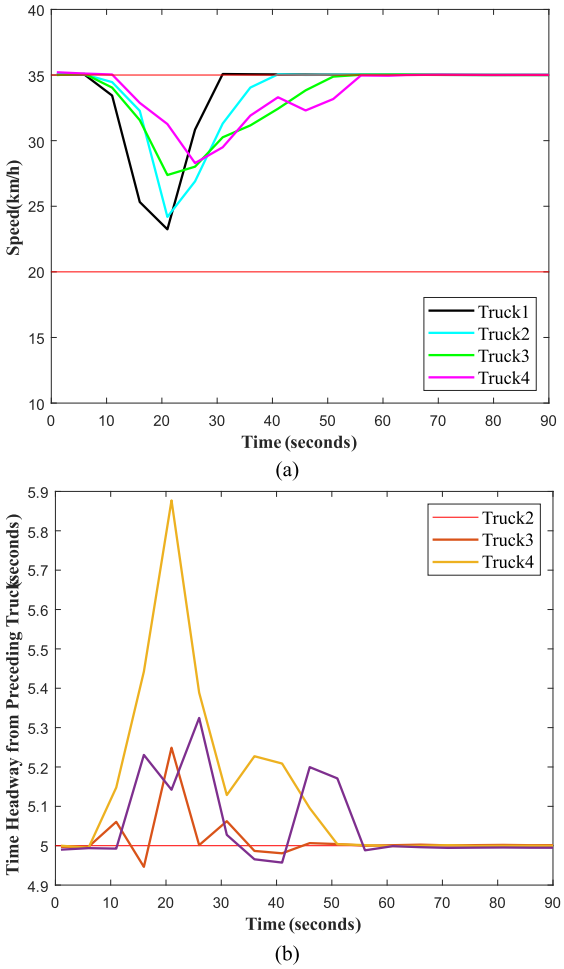

FIGURE 12. Full platoon following performance in Scenario 1.

All the KPIs are divided into three categories: the first category characterizes the performance of the truck dynamics model, including *speed error at time t* and *speed error at distance s*. The first one indicates the dynamic response speed of the dynamics model, while the second one reflects the

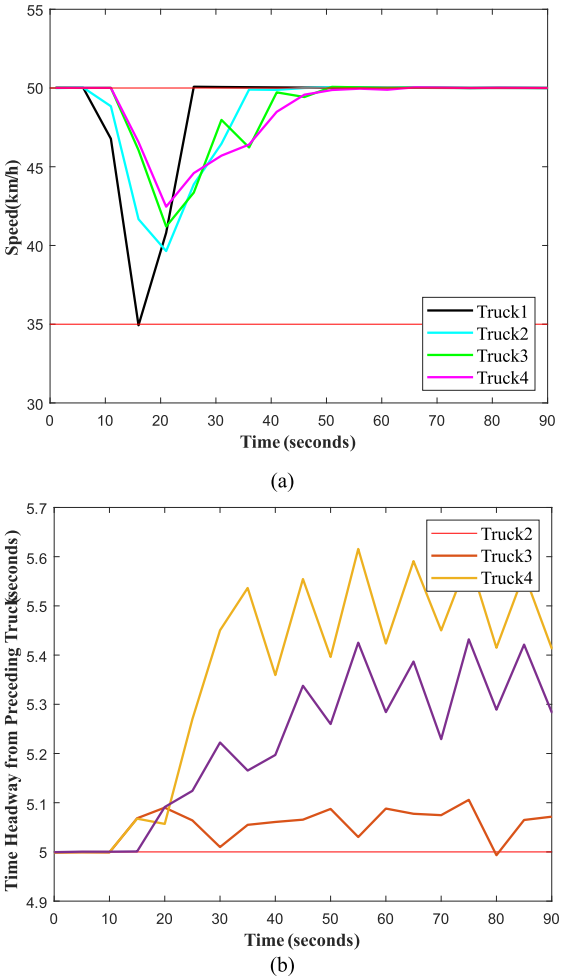

FIGURE 13. Empty platoon following performance in Scenario 1.

accuracy of the trajectory tracking of the dynamics model, which has a direct impact on the efficiency and energy consumption of the truck during operation. The second category characterizes the stability of the FP and includes the time headway from the proceeding truck, which ensures the safety of the fleet operation. That is, the algorithm always ensures that the time headway between trucks is greater than the minimum time headway when the platoon is stable. The third category characterizes the efficiency of the fleet production operation process, including *distance delay* and *time delay*. Since the reference trajectory is obtained from the operation schedule, it ensures the optimization of the fleet production efficiency. Therefore, the smaller the time delay and distance delay are, the closer the fleet production efficiency is to the optimization goal.

IV. RESULT

A. EV DYNAMIC SPEED TRAJECTORY FOLLOWING PERFORMANCE

Fig. 9 shows the following results of the electric truck dynamics model for the custom speed trajectory in Fig. 8. Under the no-load condition, the actual acceleration of the model

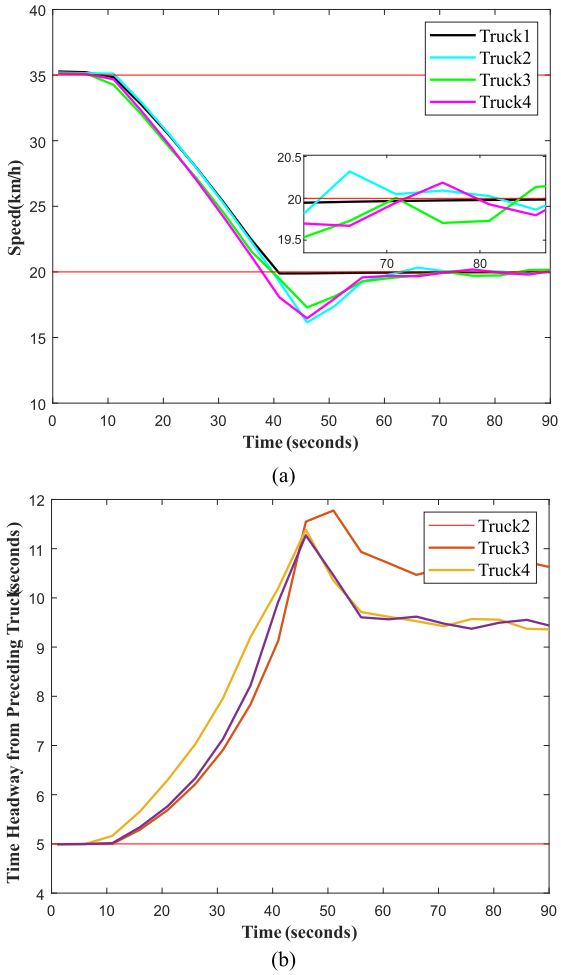

FIGURE 14. Full platoon following performance in Scenario 2.

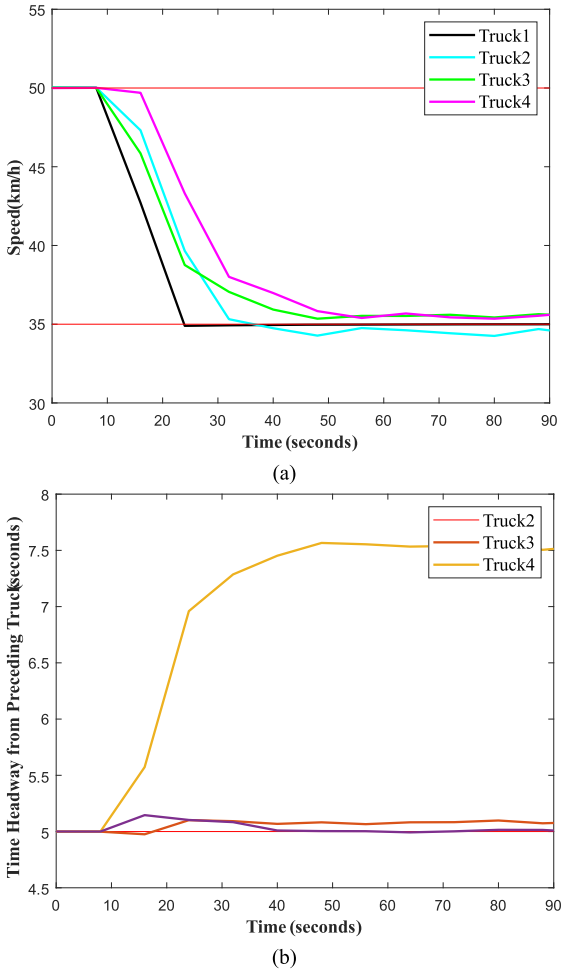

FIGURE 15. Empty platoon following performance in Scenario 2.

is less than the desired speed trajectory when the speeds are greater than 35 km/h and the acceleration is $a = 0.8\text{m/s}^2$, resulting in the actual speed being less than the desired speed, with a maximum error of 4.5 km/h (1.25 m/s). For the rest of the conditions, the speed error is within 1km/h (0.28 m/s). Under the full load condition, when the speed is greater than 20km/h and the acceleration is set to $a = 0.4\text{m/s}^2$, the speed error is 2 km/h (0.56 m/s). At beginning of the truck entering the ramp, the speed error is also 2km/h (0.56 m/s), and then the error gradually decreases. The speed error in the rest of the conditions is within 1km/h (0.28 m/s).

Figs. 10 and 11 show the simulation results of the optimal speed trajectory following of the electric mining truck in the path network under no-load and full-load optimal speed trajectory following performance with no load conditions, respectively. In the process of no-load transportation, the speed error increases gradually during the first 50 meters of the beginning stage, i.e., during the speed from 0 to the maximum speed, and the maximum speed error is 2.3 m/s. After that, the speed error decreases and remains within 0.5 m/s. The actual travel time is less than 1 s ahead of the optimal speed trajectory travel time. The full-load transportation process is similar to the no-load transportation process, except for the starting phase, the speed error is always kept within 1 m/s, and the travel time error is within 1s. In summary, we believe that the model can better simulate the actual operation of an electric mining truck.

B. PLATOON FOLLOWING STABILITY PERFORMANCE

Figs. 12 to 15 show the actual speed of the platoon and the time headway between the following truck and the preceding truck in the prescribed 4 experiments. In all 4 experiments, the initial time headway is set to 5 s, Truck 0 is the leading truck, and Trucks 2 to 4 are following trucks.

In the experiments of Scenario 1, when the speed of the leading truck suddenly decreases, the following trucks will also start to slow down in sequence. After the leading truck begins to accelerate to its original speed, the following trucks also gradually return and stabilize to their original speed. Among the three following trucks, the higher the priority of the truck is, the earlier it begins to decelerate due to the influence of the leading truck, the earlier it begins to reaccelerate, and the greater the deceleration amplitude, as shown in Figs. 12(a) and 13(a). During the operation of the platoon,

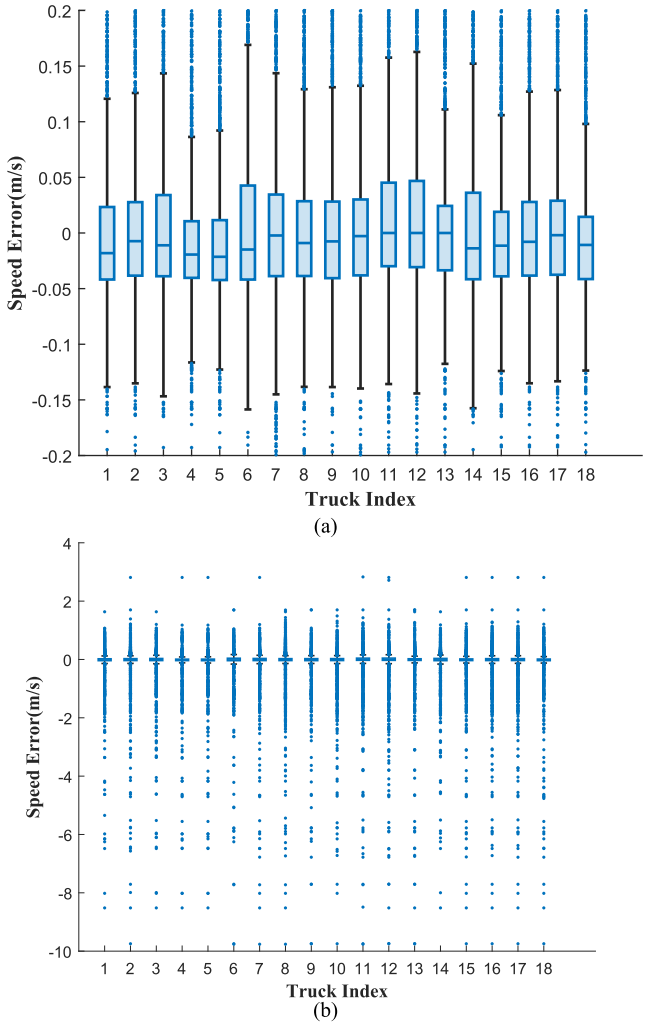

FIGURE 16. Speed error distribution of different trucks in the production process.

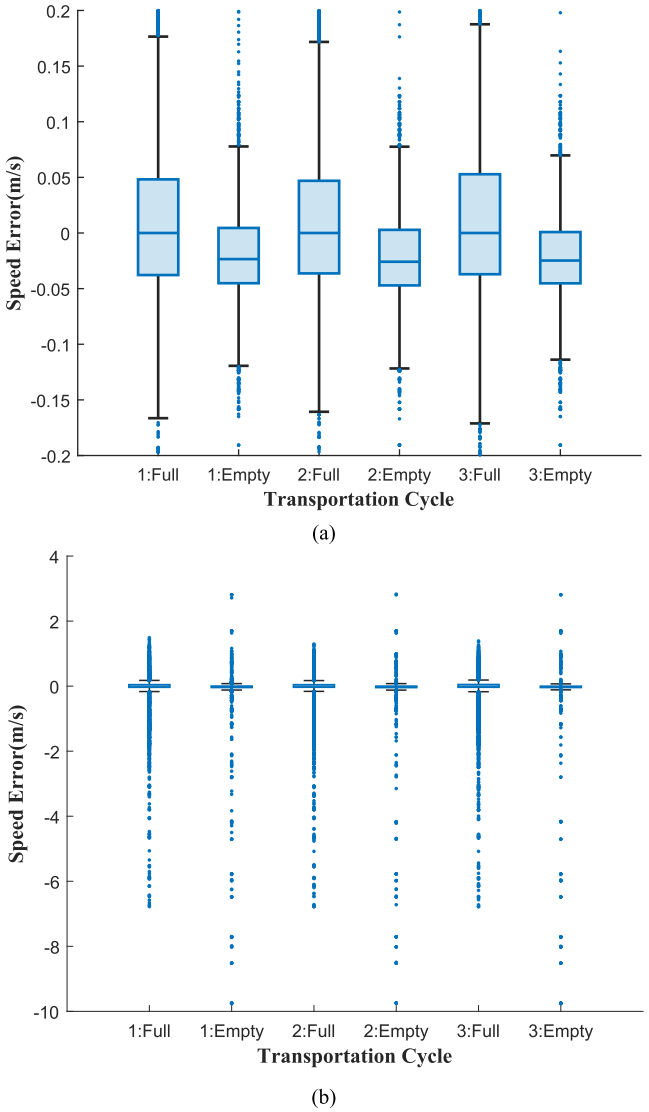

FIGURE 17. Speed error distribution of different transportation cycles in the production process.

the initial time headway is 5 s. As the platoon begins to slow down, the time headway slightly increases. When the platoon returns to the original speed, the time headway returns to approximately 5 s, as shown in Figs. 12(b) and 13(b).

In the experiments of Scenario 2, after the leading truck begins to slow down, the following trucks also begin to slow down, and the speed eventually stabilizes within 0.5 km/h (full platoon) to 1 km/h (empty platoon) of the leading truck's actual speed, as shown in Figs. 14(a) and 15(a). In Figs. 14(b) and 15(b), it can be seen that the time headway in the platoon increases to varying degrees as the trucks' speed decreases, ensuring the safety of the fleet's operation.

Therefore, it can be seen that when the speed of the preceding truck suddenly decreases during the operation of the platoon with 2 different scenarios, the algorithm can adjust the speed of the following truck and stabilize it at the speed of the preceding truck to ensure safe spacing and keep it stable. It can also be concluded that when the following truck is catches up with the preceding truck and is close to the minimum safe headway, the algorithm can also reduce the speed of the following truck to maintain the stability of the platoon operation. Compared with the previous work in [43], the following trucks will eventually stabilize to their original speed. However, in this paper, when the leading truck reach the target speed, it takes nearly 30 s for all following trucks to stabilize at the target speed, and the time headway becomes larger in Scenario 2, while the controller proposed in the literature [43] takes only 5 s to achieve the final state, and the time headway stays the same in all scenarios. The reason for the large response gap is related to the accuracy of the EV dynamics model, the control performance of the controller, and the difference in the dynamic characteristics of mining trucks and passenger cars.

C. FLEET PRODUCTION SIMULATION

Fig. 16 shows the speed following error distribution of different trucks in the fleet during the production process. More than half of the time, the speed error of the fleet stays within 0.05 m/s (subfigure(a)), and only a very few times does the

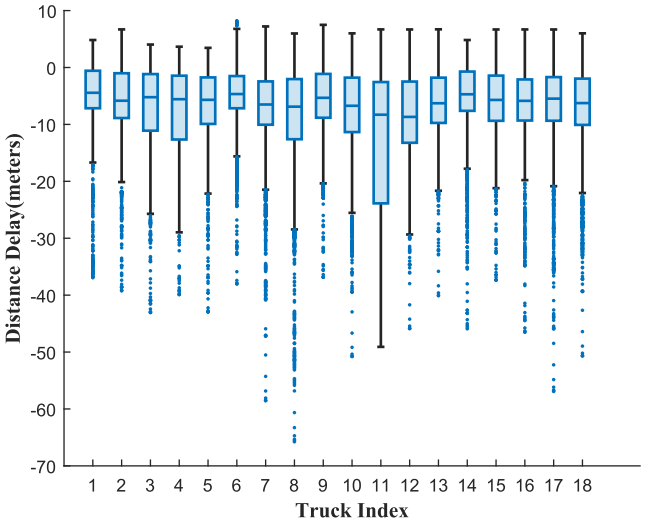

FIGURE 18. Distance delay distribution of different trucks in the production process.

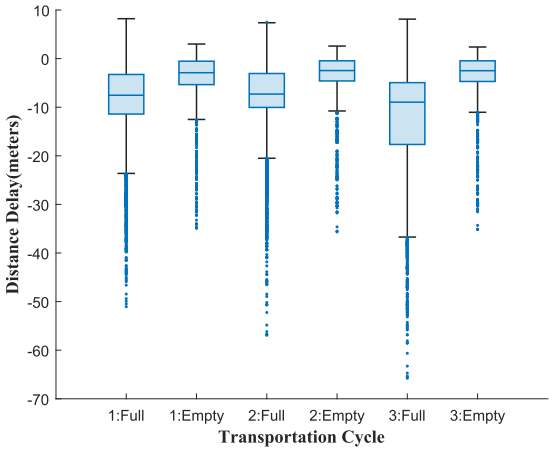

FIGURE 19. Distance delay distribution of different transportation cycles in the production process.

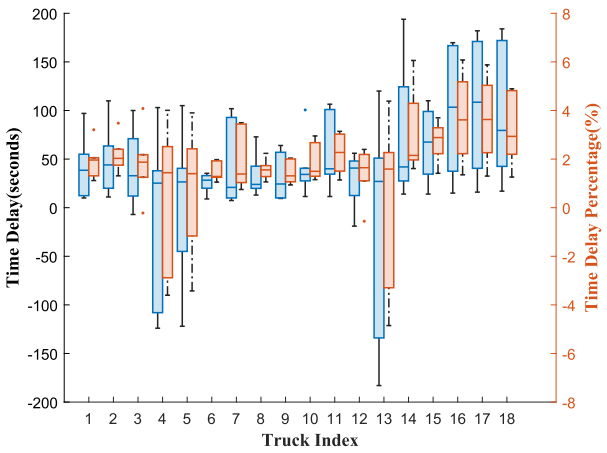

FIGURE 20. Time delay distribution of different trucks in the production process.

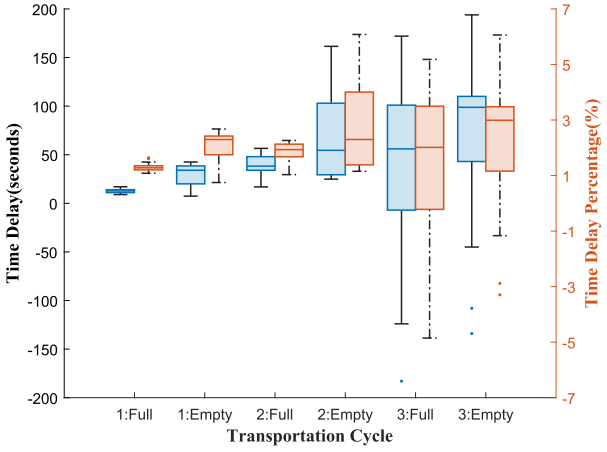

FIGURE 21. Time delay distribution of different transportation cycles in the production process.

speed error exceed 2 m/s (subfigure(b)). It can be seen that the speed following of the fleet is more stable, and the distribution of speed errors does not differ significantly between trucks. Fig. 17 shows the distribution of fleet speed following errors in different cycles during the whole production process. The loading status has a large impact on the overall truck mass, so the distribution of the truck in following speed error is significantly correlated with the loading status, and the fleet speed following error is generally smaller and more concentrated when it is empty than when it is fully loaded.

Figs. 18 and 19 show the distribution of the fleet tracking distance error throughout the transportation process among different trucks and different transportation cycles, respectively. In Fig. 18, almost all trucks have a distance tracking error within 10 m for more than half of the shift time. However, there is a difference in the distribution of distance error among different trucks. The main source of this variation is due to the different priorities of different trucks in the platoon. When a truck is the leading truck (e.g., trucks 1, 9, 14), it is not affected by other trucks in the same FP and therefore generates less potential traffic conflicts and therefore fewer travel delay, with a maximum travel delay of 40 m to 50 m.

Fig. 20 illustrates the distribution of the completion time between different trucks in the fleet. Fig. 21 illustrates the distribution of the completion time between different transportation cycles. In Figs. 10 and 11, we learned that the completion time of a single transport task is slightly ahead of the optimal speed trajectory when the trucks are not affected by others. In Fig. 20, trucks 4, 5 and 13, as the earliest trucks departing from different loading sites after the start of the shift, have been unaffected by other trucks, so these three trucks can complete their desired transport tasks ahead of schedule. Conversely, the remains are affected by their preceding truck departures, so there is a different degree of time delay for them. The later the start of the shift, the greater the influence from other trucks and the greater the time delay.

In Fig. 21, the completion time delay or advance of the fleet also gradually increases as the transportation cycle increases, from less than 20 s in the first cycle to 200 s in the last cycle, as well as for all trucks. However, overall, the percentage of time delayed by the fleet does not increase significantly and always stays within 5% of the total operation time.

V. CONCLUSION AND FURTHER WORK

In this paper, we propose a sequential distributed model predictive control algorithm (DMPC) for solving the control problem of an automated mining transportation fleet. The algorithm uses the fleet operating schedule obtained from the dispatching system as a reference, and the second-order dynamics model of the electric mining truck is controlled with the objective of minimizing the deviation between the actual state of the truck and the operating schedule. To evaluate the effectiveness of our proposed algorithm, we simulated the stability of the fleet following operation and fleet production processes, while verifying the validity of the electric truck dynamics model. The remarkable conclusions and further research directions of implementing the proposed sequential DMPC algorithm in the case study are as follows:

1) A second-order electric truck dynamic model is built and validated to be controlled as the actuators. The speed error of the model remains within 0.2 m/s under steady-state operating conditions, and increases to 2 m/s only when the operating conditions change.

2) Our proposed algorithm can guarantee the stability of the platoon's safe spacing. When the leading truck changes the target speed, it takes nearly 30 s for all following trucks to stabilize at the target speed, and the time headway becomes larger in Scenario 2.

3) During the fleet production and transportation process, the algorithm ensures that the fleet runs according to the fleet operation schedule within a reasonable error margin. Over three fourths of the operation time, the speed error of the fleet is within 0.2m/s, and the distance delay is within 40 m, with a maximum of less than 70 m, accounting for less than 0.05% of the total operating mileage. The maximum time delay is approximately 180 s, accounting for 5% of the total transportation time. Moreover, the priority of trucks in the platoon has a direct impact on operation delays, and the lower the priority is, the greater the resulting delay.

4) Compared to the existing passenger car controller, the controller proposed in this paper makes the platoon reach the steady state more slowly, but the reason for this phenomenon is not clear due to the large number of influencing factors. In our future work, we will investigate this issue.

5) It is necessary to add terminal constraints to the objective function for the asymptotic stability of the SEQ_DMPC algorithm proposed in this paper.

REFERENCES

[1] X. Wang, Q. Dai, Y. Bian, G. Xie, B. Xu, and Z. Yang, "Real-time truck dispatching in open-pit mines," *Int. J. Mining, Reclamation Environ.*, vol. 37, pp. 504–523, Apr. 2023, doi: 10.1080/17480930.2023.2201120.

[2] S. Benlaajili, F. Moutaouakkil, A. Chebak, H. Medromi, L. Deshayes, and S. Mourad, "Optimization of truck-shovel allocation problem in open-pit mines," in *Smart Applications and Data Analysis* (Communications in Computer and Information Science), vol. 1207, M. Hamlich,L. Bellatreche, A. Mondal, and C. Ordonez, Eds. Cham, Switzerland: Springer, 2020, pp. 243–255, doi: 10.1007/978-3-030-45183-7_19.

[3] K. Guo, J. Zhu, and L. Shen, "An improved acceleration method based on multi-agent system for AGVs conflict-free path planning in automated terminals," *IEEE Access*, vol. 9, pp. 3326–3338, 2021, doi: 10.1109/ACCESS.2020.3047916.

[4] Y. Zhang, C. Yang, K. Tang, and J. Dai, "Study on distributed consistent cooperative control of multi-ART in automated container terminals," *IEEE Access*, vol. 10, pp. 122965–122980, 2022, doi: 10.1109/ACCESS.2022.3223360.

[5] Z. Zhang, Q. Guo, J. Chen, and P. Yuan, "Collision-free route planning for multiple AGVs in an automated warehouse based on collision classification," *IEEE Access*, vol. 6, pp. 26022–26035, 2018, doi: 10.1109/ACCESS.2018.2819199.

[6] R. Xu, H. Feng, J. Liu, and W. Hong, "Dynamic spare point application based coordination strategy for multi-AGV systems in a WIP warehouse environment," *IEEE Access*, vol. 10, pp. 80249–80263, 2022, doi: 10.1109/ACCESS.2022.3195173.

[7] E. Mejri, S. Kelouwani, Y. Dubé, N. Henao, and K. Agbossou, "Energy efficient order picking routing for a pick support automated guided vehicle (Ps-AGV)," *IEEE Access*, vol. 10, pp. 108832–108847, 2022, doi: 10.1109/ACCESS.2022.3212797.

[8] H. Tang, X. Cheng, W. Jiang, and S. Chen, "Research on equipment configuration optimization of AGV unmanned warehouse," *IEEE Access*, vol. 9, pp. 47946–47959, 2021, doi: 10.1109/ACCESS.2021.3066622.

[9] J. Xun, M. Chen, Y. Liu, and F. Liu, "An overspeed protection mechanism for virtual coupling in railway," *IEEE Access*, vol. 8, pp. 187400–187410, 2020, doi: 10.1109/ACCESS.2020.3029147.

[10] B. Chen, R. Zhang, F. Zhou, and W. Du, "An observer-driven distributed consensus braking control method for urban railway trains with unknown disturbances," *Actuators*, vol. 12, no. 3, p. 111, Mar. 2023, doi: 10.3390/act12030111.

[11] G. Marlière, S. Sobieraj Richard, P. Pellegrini, and J. Rodriguez, "A conditional time-intervals formulation of the real-time railway traffic management problem," *Control Eng. Pract.*, vol. 133, Apr. 2023, Art. no. 105430, doi: 10.1016/j.conengprac.2022.105430.

[12] M. R. Hidayatullah and J.-C. Juang, "Centralized and distributed control framework under homogeneous and heterogeneous platoon," *IEEE Access*, vol. 9, pp. 49629–49648, 2021, doi: 10.1109/ACCESS.2021.3068968.

[13] F. Jaffar, T. Farid, M. Sajid, Y. Ayaz, and M. J. Khan, "Prediction of drag force on vehicles in a platoon configuration using machine learning," *IEEE Access*, vol. 8, pp. 201823–201834, 2020, doi: 10.1109/ACCESS.2020.3035318.

[14] S. E. Shladover, C. A. Desoer, J. K. Hedrick, M. Tomizuka, J. Walrand, W.-B. Zhang, D. H. Mcmahon, H. Peng, S. Sheikholeslam, and N. McKeown, "Automated vehicle control developments in the PATH program," *IEEE Trans. Veh. Technol.*, vol. 40, no. 1, pp. 114–130, Feb. 1991, doi: 10.1109/25.69979.

[15] K. B. Devika, G. Rohith, V. R. S. Yellapantula, and S. C. Subramanian, "A dynamics-based adaptive string stable controller for connected heavy road vehicle platoon safety," *IEEE Access*, vol. 8, pp. 209886–209903, 2020, doi: 10.1109/ACCESS.2020.3039797.

[16] F. Gao, S. E. Li, Y. Zheng, and D. Kum, "Robust control of heterogeneous vehicular platoon with uncertain dynamics and communication delay," *IET Intell. Transp. Syst.*, vol. 10, no. 7, pp. 503–513, Sep. 2016, doi: 10.1049/iet-its.2015.0205.

[17] D. Yanakiev and I. Kanellakopoulos, "Nonlinear spacing policies for automated heavy-duty vehicles," *IEEE Trans. Veh. Technol.*, vol. 47, no. 4, pp. 1365–1377, Nov. 1998, doi: 10.1109/25.728529.

[18] K.-Y. Liang, J. Mårtensson, and K. H. Johansson, "Heavy-duty vehicle platoon formation for fuel efficiency," *IEEE Trans. Intell. Transp. Syst.*, vol. 17, no. 4, pp. 1051–1061, Apr. 2016, doi: 10.1109/TITS.2015.2492243.

[19] R. Zheng, K. Nakano, S. Yamabe, M. Aki, H. Nakamura, and Y. Suda, "Study on emergency-avoidance braking for the automatic platooning of trucks," *IEEE Trans. Intell. Transp. Syst.*, vol. 15, no. 4, pp. 1748–1757, Aug. 2014, doi: 10.1109/TITS.2014.2307160.

[20] Q. Zhao, H. Zheng, C. Kaku, F. Cheng, and C. Zong, "Safety spacing control of truck platoon based on emergency braking under different road conditions," *SAE Int. J. Vehicle Dyn., Stability, NVH*, vol. 7, no. 1, pp. 1–5, Oct. 2022, doi: 10.4271/10-07-01-0005.
[21] D. Swaroop, J. K. Hedrick, C. C. Chien, and P. Ioannou, "A comparision of spacing and headway control laws for automatically controlled vehicles," *Vehicle Syst. Dyn.*, vol. 23, no. 1, pp. 597–625, Jan. 1994, doi: 10.1080/00423119408969077.
[22] X. Guo, J. Wang, F. Liao, and R. S. H. Teo, "Distributed adaptive integrated-sliding-mode controller synthesis for string stability of vehicle platoons," *IEEE Trans. Intell. Transp. Syst.*, vol. 17, no. 9, pp. 2419–2429, Sep. 2016, doi: 10.1109/TITS.2016.2519941.
[23] D. Pi, P. Xue, B. Xie, H. Wang, X. Tang, and X. Hu, "A platoon control method based on DMPC for connected energy-saving electric vehicles," *IEEE Trans. Transport. Electrific.*, vol. 8, no. 3, pp. 3219–3235, Sep. 2022, doi: 10.1109/TTE.2022.3155493.
[24] G. Guo and W. Yue, "Hierarchical platoon control with heterogeneous information feedback," *IET Control Theory Appl.*, vol. 5, no. 15, pp. 1766–1781, Oct. 2011, doi: 10.1049/iet-cta.2010.0765.
[25] A. Bozzi, S. Graffione, C. Pasquale, R. Sacile, S. Sacone, and S. Siri, "A hierarchical control scheme to improve the travel performance of truck platoons in freeways," in *Proc. IEEE 25th Int. Conf. Intell. Transp. Syst. (ITSC)*, Oct. 2022, pp. 2063–2068, doi: 10.1109/ITSC55140.2022.9922170.
[26] V. Turri, B. Besselink, and K. H. Johansson, "Cooperative look-ahead control for fuel-efficient and safe heavy-duty vehicle platooning," *IEEE Trans. Control Syst. Technol.*, vol. 25, no. 1, pp. 12–28, Jan. 2017, doi: 10.1109/TCST.2016.2542044.
[27] D. Swaroop and J. K. Hedrick, "Constant spacing strategies for platooning in automated highway systems," *J. Dyn. Syst., Meas., Control*, vol. 121, no. 3, pp. 462–470, Sep. 1999, doi: 10.1115/1.2802497.
[28] P. Seiler, A. Pant, and K. Hedrick, "Disturbance propagation in vehicle strings," *IEEE Trans. Autom. Control*, vol. 49, no. 10, pp. 1835–1841, Oct. 2004, doi: 10.1109/TAC.2004.835586.
[29] Y. Zheng, S. E. Li, K. Li, F. Borrelli, and J. K. Hedrick, "Distributed model predictive control for heterogeneous vehicle platoons under unidirectional topologies," *IEEE Trans. Control Syst. Technol.*, vol. 25, no. 3, pp. 899–910, May 2017, doi: 10.1109/TCST.2016.2594588.
[30] Y. Zheng, S. E. Li, K. Li, and W. Ren, "Platooning of connected vehicles with undirected topologies: Robustness analysis and distributed H-infinity controller synthesis," *IEEE Trans. Intell. Transp. Syst.*, vol. 19, no. 5, pp. 1353–1364, May 2018, doi: 10.1109/TITS.2017.2726038.
[31] W. Wang, "The safety and comfort control of vehicles by the separation principle of PID controller tuning," in *Proc. IEEE Int. Conf. Ind. Technol.*, Via del Mar, Chile, Mar. 2010, pp. 145–150, doi: 10.1109/ICIT.2010.5472668.
[32] N. Pourmohammad-Zia, F. Schulte, R. G. González-Ramírez, S. Voß, and R. R. Negenborn, "A robust optimization approach for platooning of automated ground vehicles in port hinterland corridors," *Comput. Ind. Eng.*, vol. 177, Mar. 2023, Art. no. 109046, doi: 10.1016/j.cie.2023.109046.
[33] A. Zhou, S. Peeta, M. Yang, and J. Wang, "Cooperative signal-free intersection control using virtual platooning and traffic flow regulation," *Transp. Res. C, Emerg. Technol.*, vol. 138, May 2022, Art. no. 103610, doi: 10.1016/j.trc.2022.103610.
[34] M. Xiaoxiang, T. Zhimin, and C. Feng, "A reliability-based approach to evaluate the lateral safety of truck platoon under extreme weather conditions," *Accident Anal. Prevention*, vol. 174, Sep. 2022, Art. no. 106775, doi: 10.1016/j.aap.2022.106775.
[35] C. Zhai, F. Luo, Y. Liu, and Z. Chen, "Ecological cooperative look-ahead control for automated vehicles travelling on freeways with varying slopes," *IEEE Trans. Veh. Technol.*, vol. 68, no. 2, pp. 1208–1221, Feb. 2019, doi: 10.1109/TVT.2018.2886221.
[36] J. Richalet, A. Rault, J. L. Testud, and J. Papon, "Model predictive heuristic control: Applications to industrial processes," *Automatica*, vol. 14, no. 5, Sep. 1978, pp. 413–428, doi: 10.1016/0005-1098(78)90001-8.
[37] D. Jia and B. Krogh, "Distributed model predictive control," in *Proc. Amer. Control Conf.*, vol. 4, Feb. 2001, pp. 2767–2772, doi: 10.1109/ACC.2001.946306.
[38] R. Kianfar, P. Falcone, and J. Fredriksson, "A receding horizon approach to string stable cooperative adaptive cruise control," in *Proc. 14th Int. IEEE Conf. Intell. Transp. Syst. (ITSC)*, Washington, DC, USA, Oct. 2011, pp. 734–739, doi: 10.1109/ITSC.2011.6083088.
[39] R. Kianfar, P. Falcone, and J. Fredriksson, "A distributed model predictive control approach to active steering control of string stable cooperative vehicle platoon," *IFAC Proc. Volumes*, vol. 46, no. 21, pp. 750–755, 2013, doi: 10.3182/20130904-4-JP-2042.00040.
[40] L. Dai, Q. Cao, Y. Xia, and Y. Gao, "Distributed MPC for formation of multi-agent systems with collision avoidance and obstacle avoidance," *J. Franklin Inst.*, vol. 354, no. 4, pp. 2068–2085, Mar. 2017, doi: 10.1016/j.jfranklin.2016.12.021.
[41] V. M. Zavala and A. Flores-Tlacuahuac, "Stability of multiobjective predictive control: A utopia-tracking approach," *Automatica*, vol. 48, no. 10, pp. 2627–2632, Oct. 2012, doi: 10.1016/j.automatica.2012.06.066.
[42] P. D. Christofides, R. Scattolini, D. M. de la Peña, and J. Liu, "Distributed model predictive control: A tutorial review and future research directions," *Comput. Chem. Eng.*, vol. 51, pp. 21–41, Apr. 2013, doi: 10.1016/j.compchemeng.2012.05.011.
[43] E. Kayacan, "Multiobjective H_∞ control for string stability of cooperative adaptive cruise control systems," *IEEE Trans. Intell. Vehicles*, vol. 2, no. 1, pp. 52–61, Mar. 2017, doi: 10.1109/TIV.2017.2708607.

ZHICHAO WANG received the B.S. degree in vehicle engineering from the University of Science and Technology Beijing, Beijing, China, in 2018, where he is currently pursuing the Ph.D. degree in mechanical engineering.

His research interests include nonlinear dynamic control, modeling of hybrid powertrain and autonomous driving with mining heavy trucks, and real-time dispatching and cooperative control for heavy truck platoon.

JUE YANG received the B.S. degree in mechanical engineering from Yanshan University, Qinhuangdao, China, in 1997, and the Ph.D. degree in vehicle engineering from the University of Science and Technology Beijing, Beijing, China, in 2005. He is currently a Professor with the School of Mechanical Engineering, University of Science and Technology Beijing, and the Director of the Department of Vehicle Engineering. His research interests include nonlinear dynamic and control, heavy vehicle design and control, autonomous driving with mining vehicles, and modeling of hybrid powertrains.